Gold mineralization and metallogenesis associated with mantle dynamics in East China

Chuansong He[1]

Institute of Geophysics, China Earthquake Administration, Beijing 100081, China

Abstract: East China can be divided into two parts: the North China Block (or North China Craton) (NCC) and the South China Block (SCB). The mechanism for the destruction of the NCC and the large-scale magmatic activity in the SCB during the Mesozoic is a major focus in the geosciences; however, related scientific issues, such as gold mineralization in the NCC and the metallogenesis in the SCB, remain enigmatic. Recently, receiver function analysis and tomography have been used to define the vestiges of an upwelling mantle plume beneath the NCC and large-scale mantle upwelling beneath the SCB in the Mesozoic. In this study, the dynamic processes of the mantle plume and upwelling mantle are analysed, and the relationships between the mantle plume and gold mineralization as well as between mantle upwelling and metallogenesis are discussed. Finally, it is suggested that gold mineralization in the NCC might be linked to a Mesozoic mantle plume while metallogenesis in the SCB might be related to Mesozoic mantle upwelling.

Keywords: Upwelling mantle plume, Mantle upwelling, Gold mineralization, Metallogenesis, North China Craton, South China Block.

Plain language summary:

In this study, newest seismic studies indicated that there is upwelling mantle plume in the North China Craton (NCC) and mantle upwelling in the South China Block (SCB). Through comprehensive analysis. It is suggested that that gold mineralization in the NCC might be linked to a Mesozoic mantle plume while metallogenesis in the SCB might be related to Mesozoic mantle upwelling.

1. Introduction

1.1. Geological background of the NCC

The NCC is bounded by the late Palaeozoic to Mesozoic Central Asian orogen in the north, the early Palaeozoic Qilian orogen in the west, and the Mesozoic Qinling–Dabie–Sulu orogen in the south (Zhao et al., 2001). During the Paleoproterozoic between 1.92 and 1.85 Ga, the Ordos and Yinshan Blocks were amalgamated along the Inner Mongolia suture zone, forming the unified Western Block (Zhao and Zheng, 2005), and the Eastern and Western Blocks collided along the Trans-North China orogen (Zhao and Zhai, 2013) (Fig. 1a, red rectangular region, Fig. 1b).

The thick, old and refractory lithospheric keel is widely accepted to have been largely replaced by fertile and young lithospheric mantle beneath the eastern

[1]* Corresponding author. hechuansong@aliyun.com (C.S.H)

part of the NCC during the Mesozoic and Cenozoic (Wu et al., 2019; Zhao et al., 2020), which implies lithospheric thinning or destruction of the NCC (Zhai et al., 2007). Models of craton destruction in the NCC involve two schools of thought: one proposes that lower crustal and/or lithospheric delamination resulted in lithospheric thinning or craton destruction (Liu et al., 2019; He, 2020), and the other suggests that upwelling asthenosphere led to thermal or mechanical erosion beneath the lithosphere and ultimately craton destruction (Zhang et al., 2002).

Geologists have studied the abundant gold deposits generated by the destruction of the NCC, which was accompanied by widespread crustal/lithospheric deformation and magmatic activity (Yang et al., 2003). In particular, the consistency between the time of lithospheric thinning and the ages of most gold ores in the NCC suggests that the destruction of the craton exerted a major control on gold mineralization in the late Mesozoic (Li et al., 2013).

1.2. Geological background of the South China Block

The SCB is composed of the Cathaysia and Yangtze Blocks, which are assembled along the Jiujiang-Shitai fault (He et al., 2013). The SCB was formed by collision of the Yangtze and Cathaysia subblocks at approximately 0.8–1 Ga along the Jiangnan orogen or the Jiujiang-Shitai fault, which shaped its fundamental tectonic architecture (Yao et al., 2011; He et al., 2013) (Fig. 1a, blue rectangular region; Fig. 1c). Following this event, the SCB further docked with the NCC to the north along the Qinling–Tongbai–Hong'an–Dabie–Sulu orogenic belt, to the west along the Longmenshan fault and to the southwest along the Ailaoshan-Song Ma orogen with the Indochina Block in the Triassic (Zheng et al., 2013).

The SCB basement is dominantly composed of Paleoproterozoic, Mesoproterozoic and early Neoproterozoic rocks (Zhao and Zheng, 2009) that were involved in and overprinted by at least three tectonic events, namely, the Caledonian in the early Palaeozoic, Indosinian in the Triassic and Yanshanian during the Jurassic-Cretaceous (e.g., Charvet, 2013), which might have led to the inhomogeneous rejuvenation of ancient crustal and lithospheric structures (e.g., Li et al., 2012). Concurrently, the SCB retains the imprints of several metallogenic and tectonothermal events that correspond to global supercontinental cycles and tectonic activity and is one of the major polymetallic provinces in the world.

1.3. Scientific background and aims of this study

A number of studies have speculated that upwelling mantle plumes are generally rich in Au (e.g., Sisson et al., 2003; Webber et al. 2013), which can lead to globally different styles of Au mineralization, such as Carlin-type deposits in the US (e.g., Oppliger et al. 1997) and China (Zhu et al. 2020) and porphyry deposits in South America (e.g., Tassara et al. 2017). However, it is not clear how the upwelling mantle plume leads to Au mineralization. Recently, receiver function and tomography (Lei, 2012, He, 2020) have defined a vestige of an upwelling Mesozoic mantle plume beneath the NCC that corresponds well

to the region of gold mineralization, which implies that the upwelling mantle plume may be related to the gold mineralization in this area. In this study, the dynamic process of the upwelling mantle plume is analysed in the NCC, and the relationship between the upwelling mantle plume and gold mineralization is discussed. Finally, it is proposed that the upwelling mantle plume might lead to gold mineralization in the NCC.

Although many researchers have considered that magmatism may be related to the formation of the polymetallic province in the SCB (e.g., Deng et al., 2014), it is not clear what generated the large-scale magmatism and how it induced the metallogeny in the SCB. Recently, receiver function analysis and tomography have revealed a vestige of the large-scale mantle upwelling beneath the SCB in the Mesozoic (He and Santosh, 2016, 2021) that corresponds well to the Mesozoic magmatism and metallogeny region in the SCB, which implies that mantle upwelling may have resulted in the large-scale magmatism and metallogeny in the SCB. However, the relationship between the mantle upwelling and metallogeny need to be further clarified. In this study, a thorough examination of the tectonic evolution and a detail analysis of the mantle upwelling are carried out in this area. Finally, it is suggested that the mantle upwelling might have led to large-scale magmatism and resulted in the metallogeny in the Mesozoic in the SCB.

1. Data and method of receiver function and tomography

He et al. (2014) performed H-k stacking of receiver functions using 441 teleseismic events with magnitude mb 5.8 recorded by 314 seismic stations. For each event-station pair, data were selected within the ranges of 30°-95° and initially windowed 15 *s* before and 120 *s* after the *P*-wave pick. Data were filtered using a zero-phase Butterworth bandpass filter with corner frequencies of 0.03-3 *Hz*. A modified frequency domain deconvolution was carried out, and the Gaussian factor and water level were set to 3 and 0.01. One of the results indicates that the bulk *Vp/Vs* ratio identified in this study show higher values for the regions in the northern part of the eastern NCC and the Trans-North China Orogen (>1.76) than for other regions, which might represent mafic and ultramafic lower crust. This implies that an upwelling mantle plume led to lower crustal underplating and magma intrusion in this region.

He (2020) used 647 teleseismic events recorded by the China Earthquake Network with 671 seismic stations from July 2007 to March 2014 and data from the Incorporated Research Institutions for Seismology (IRIS) to carry out tomography and common conversion point (CCP) stacking of receiver functions. Seismic events with magnitudes >6.0 and epicentral distances ranging from 30°-85° were selected. Waveforms were cut from digital seismograms 15 s before and 50 s after the first P-wave arrival and filtered between 0.3 and 3 Hz. Finally, 102421 first P-wave arrivals were extracted using the time cross-correlation method. A damping value of 20.0 was selected for use in the tomographic inversion following a trade-off or L-shaped curve. One of results revealed a mushroom-like low-velocity anomaly beneath the Eastern Block of the NCC, which might be a

vestige of the upwelling mantle plume from the Mesozoic. The CCP technique was employed to stack 85,015 high-quality receiver functions and to image the mantle transition zone beneath the NCC. The results show that the location of the mantle plume corresponds well to the region where both the 410 and 660 km discontinuities become deeper.

He et al. (2013) applied H-k stacking of receiver functions in the South China Block using 424 teleseismic events recorded by 254 seismic stations; the data processing and method were similar to those of He et al. (2014). One of the results shows a region with high Vp/Vs ratio in the Cathaysia Block, which might be associated with magmatic intrusions generated by mantle upwelling.

He and Santosh (2016) collected 57813 P-wave arrivals from 449 teleseismic events recorded by 382 seismic stations with event-station epicentral distances ranging from 30° to 85° and performed tomography in the South China Block; the data processing and method were similar to those of He (2020). One of the results indicates that there is a large-scale low-velocity anomaly beneath the Cathaysia Block, which may be connected with mantle upwelling.

He and Santosh (2021) carried out CCP stacking of receiver functions in the South China Block using 1053 teleseismic events recorded by 330 permanent seismic stations of the China Seismic Network; the data processing and method were similar to those of He (2020). One of the results demonstrated that the thinning region of the mantle transition zone corresponds well to the upwelling mantle defined by He and Santosh (2016).

1. **Mantle plume upwelling and gold mineralization in the NCC**

Wilson (1963) proposed that the lithosphere moving over a stationary mantle plume or hot spot in the mantle formed the Hawaiian Islands. Generally, mantle plume upwelling is considered to originate from the core-mantle boundary (Campbell, 2005), and it can be represented as either a low-viscosity and low-density fluid injected into a high-viscosity and high-density fluid or the lighter material of the lower boundary layer upwelling into the overlying mantle (Campbell, 2005). Therefore, upwelling mantle plumes may play a key role in material transfer and convection (Morgan, 1971), and their vestiges can be retained for several million to billion years in the mantle and be detected by seismic techniques (e.g., Phillips et al., 2018). For example, the Eifel volcanic field in the North Atlantic was induced by an upwelling mantle plume between 700,000 and 10,800 years ago as revealed by a Rayleigh wave tomography (Pilidou et al., 2005) and the Ross Island (Antarctica) lava material during the Archean to early Proterozoic associated with an upwelling mantle plume has been revealed by recent global tomographic modelling (Phillips et al., 2018).

In early Earth's geological history, due to gravitational processes, lighter elements rose upwards, whereas heavier elements sank to the core-mantle boundary or into the core of Earth; examples of heavier elements include nickel, iron, silver and gold, which are mostly concentrated at the core-mantle boundary or in the core of the Earth (Trubitsyn, 2019). Mantle plumes act as channels that

connect deep-seated (or core-mantle boundary) ore-forming material with the shallow lithosphere (Santosh et al., 2009). When a mantle plume upwells, gold or other metals retained at the core-mantle boundary and in the core begin to rise (Tassara et al., 2017) in a gaseous state (Alexander, 2014; Munteen et al., 2011) together with the hot material flow of mantle plumes into the shallow mantle or the base of the lithosphere. Finally, gold or other metals are transferred through fluid and magmatic conduits and preserved in favourable structural regions, thus forming mineral deposits (Pirajno and Santosh, 2015).

Hayden and Watson (2007) and Saunders et al. (2018) also proposed that rising plumes may potentially add Au into the sub-continental lithospheric mantle (SCLM) or introduce metal to the SCLM during their final ascent. However, this process does not exclude the upwelling transport of gold or other metals in another state. Gold is more likely to be mobilized by silicate melts than hydrous fluids (Saunders et al., 2018), and the recycling of crustal materials may contribute to the placement of gold deposits (McInnes et al., 1999).

The relationship between mantle convection and surface observations plays a key role in understanding regional tectonics and related metallogenesis (Keith, 2001; Lobkovsky and Kotelkin, 2015). Seismic parameters observed in the surface, such as P- and S-wave velocities and the Vp/Vs ratio, are indicators that reflect the bulk physical properties of Earth's interior generated by convection (Fukao et al., 2009).

In the NCC, tomography and receiver function analysis have been used to define a vestige of the upwelling mantle plume (He et al., 2015; He, 2020) (for example, Fig. 2). Tomography clearly shows a low-velocity anomaly with a mushroom-like shape originating from the lower mantle beneath the Eastern Block of the NCC (Fig. 3) (He, 2020), which is consistent with the basic features of the upwelling mantle plume, i.e., a large head followed by a relatively narrow tail (Campbell, 2005; Cloetingh et al., 2013; Weis et al., 2011).

Upwelling mantle plumes can underplate in areas with lithosphere thinning (Begg et al., 2010; Griffin et al., 2013) and intrude the lower crust (e.g., Pirajno, 2007; Saunders et al., 2018) or surface (Fig. 4), causing ultramafic/mafic lower crust and increasing Vp/Vs ratios. H-k stacking of receiver function analysis indicates ultramafic/mafic lower crust (Vp/Vs>1.76) in the northern part of the NCC (red oval region) (Fig. 5) (He et al., 2015), which corresponds well to the location of the upwelling mantle plume (Fig. 3b). Meanwhile, the distribution of gold deposits (Fig. 6) corresponds well with the location of lower crustal underplating and the upwelling mantle plume in the NCC (Fig. 2 and Fig. 5).

Geologists have also suggested an upwelling Mesozoic mantle plume beneath the NCC based on indirect geochemical and isotopic evidence and speculative tectonic models; this plume may be linked with major gold mineralization in the NCC (Zhai et al., 2007). Mineralogical studies have indicated that underplating or ultramafic/mafic magma may be related to metallic or gold deposits (e.g.,

Begg et al., 2010; McInnes et al., 1999).

Therefore, it is suggested that the upwelling mantle plume may have generated lower crustal underplating and large-scale magmatism, which led to gold mineralization in the eastern part of the NCC.

1. **Mantle upwelling and metallogenesis in the South China Block**

Since the Mesozoic, the Pacific Plate has subducted beneath the Eurasian continent (Sun et al., 2007; Hall, 2012), which has considerably influenced the tectonic and geological evolution of East China (Sun et al., 2007), especially the Cathaysia Block. Subduction also induced convective circulation (or mantle upwelling) (Zhao and Ohtani, 2009).

Tomography has been used to define a large-scale low-velocity anomaly beneath the Cathaysia Block (Fig. 7), which might be linked to a vestige of Mesozoic mantle upwelling (He and Santosh, 2016) and crustal extension during the Jurassic to early Cenozoic in the SCB (Yan et al., 2011). He et al. (2013) performed a receiver function analysis and revealed two high Vp/Vs ratio regions in the Cathaysia Block (Fig. 8), which may have been generated by magmatic intrusions from mantle upwelling. The metallic deposits in the SCB show that the Nanling metal deposit zone (Fig. 9a, blue oval) corresponds to the region with high Vp/Vs ratio (blue oval) (Fig. 9b), whereas the Cretaceous Sn-W-Pb-Zn-Au-U system along the continental margin (Fig. 9a, rectangle) corresponds to another high Vp/Vs ratio zone (Fig. 9c, blue rectangle) (Fig. 9c).

Earth's geological history includes the cyclic dispersal and assembly of continental blocks or fragments within supercontinents (e.g., Meert, 2012; Nance et al., 2014). The assembly of these continental blocks or fragments into supercontinents involves the closure of intervening ocean basins and the subduction of oceanic lithosphere (Maruyama et al., 2007). The subducted slabs may extend to the lower mantle and accumulate at the core-mantle boundary (e.g., Peacock, 1996; Zhao, 2004), forming slab graveyards. Due to multiple prolonged periods of subduction and heating from the core, slab graveyards are eventually transformed into superplumes and eventually break supercontinents apart (Pirajno and Santosh, 2015; Nance et al., 2014). The process may result in a precursor stage of the metal mantle source refertilization in the SCLM derived from upwelling superplumes, which might have played in a key role in forming the large metallogenic provinces in the Earth's crust (Begg et al., 2010; Tassara et al., 2017).

Studies on the geometries of various mineral deposit types and the evolution of metallogenesis through Earth's geological history indicate that metallogenesis is broadly related to supercontinent cycles (Khomich et al., 2014; Pirajno and Santosh, 2015). The SCB, which is one of the potential polymetallic provinces in the world (Hu et al., 2010; Shellnutt, 2014), is considered to have been involved in the cycles of ancient supercontinents, including Columbia, Rodinia, Gondwana and Pangea (Cawood et al., 2013; Yin et al., 2013). From ca. 850 Ma to 730 Ma, South China rifted from the Rodinia supercontinent (e.g., Yao et

al., 2011), and this rifting process may have been contemporaneous with a major period of metallic ores ascending into the shallow mantle and the crust. The metallogenesis in the crust may have been connected with three major factors in space and time: enriched metal in the upper mantle and lower crust, transient remobilization or mantle upwelling, and favourable lithospheric plumbing structures or faults (Tassara et al., 2017).

Large-scale magmatism (or mantle upwelling) in the SCB occurred during the Mesozoic (Zhou et al., 2006) and may have induced the remobilization of metallic ore material retained in the SCLM or lower crust, which ultimately led to fluid circulation, deep-seated heat flow and crust-mantle reactivation (Goldfarb et al., 2014). This process preserved favourable ore deposits (Fig. 9a) in the shallowing crust or surface (Begg et al., 2010; Tassara et al., 2017) and may be a major cause of metallogenesis in the SCB.

In other regions of the world, similar mineral systems have been reported (Begg et al., 2010; Herzberg and O'Hara, 2002), such as the Au-bearing metasomatic vein in the Cerro Redondo peridotite xenolith, which represents re-melting from mantle domains (Tassara et al., 2017). Studies also indicated that magmatic Ni-Cu-platinum group elements and platinum group element deposits are genetically associated with metal-rich mafic or ultramafic magmas in the mantle (Begg et al., 2010), which can be produced by high-degree melting and transport of deep mantle rocks with temperatures greater than 1,500 °C at depths of 100 km or less (Herzberg and O'Hara, 2002).

1. **The difference in dynamic processes between the NCC and the SCB**

The upwelling mantle plume (a mushroom-like low-velocity anomaly) beneath the NCC originated from the lower mantle or core-mantle boundary, and its material might have included metallic ores or mafic material. The upwelling of a mantle plume can lead to lower crustal underplating (or ultramafic/mafic lower crust), where the Vp/Vs ratio is greater than 1.76 (Fig. 5). In contrast, the upwelling mantle (not a mushroom-like low-velocity anomaly) beneath the SCB was rooted from the upper mantle rather than the lower mantle, and its upwelling material might have been different from that of the upwelling mantle plume. Upwelling mantle can intrude into the crust and result in magmatism, which induces relatively high Vp/Vs ratios; however, its Vp/Vs ratio is less than 1.76 (Fig. 8b). Geological studies also suggested that a large volume of Yanshanian granitoid rocks and lesser mafic intrusion volcanic rocks formed during the Jurassic-Cretaceous in the SCB (Sun, 2006; Deng et al., 2014), which is different from the products of the upwelling mantle plume. Accordingly, there is a great difference between the gold mineralization in the NCC and the metallogenesis in the SCB due to the difference in the dynamic processes.

1. **Conclusion**

Credible seismic evidence indicates that a vestige of a Mesozoic mantle plume remains beneath the Eastern Block of the NCC, and it corresponds well to

the distribution of gold deposits in the NCC. Credible seismic evidence also corroborates that a vestige of Mesozoic mantle upwelling occurs beneath the Cathaysia Block that is related to the Mesozoic metallogenesis in the SCB. Therefore, mantle plume upwelling might have been a major cause for the gold deposits in the NCC, whereas the metallogenesis in the SCB may have been associated with mantle upwelling. Based on these results, it is suggested that mantle dynamics might have played a key role in the gold mineralization and metallogeny. These findings are very important for understanding metallogeny around the world, which need to be studied in more detail in the future.

Acknowledgements

I would like to thank the National Key R&D Plan of China (2017YFC0601406). The travel time data used in previous studies can be accessed via http://doi.org/10.5281/zenodo.4267092.

Compliance with ethical standards

Conflict of interest: The author declares that he has no conflicts of interest.

References

Alexander, V., 2014, Thermo-Electrochemical Processes of the Earth's Degassing Creating Geomagnetic Field and Changing Its Value and Direction (Thermodynamic Approach): Int. J. Geosci., **5**, 1219-1230.

Begg, G. R., C. Hronsky, J. A. M., Arndt, N. T., Grffin, W. L., O'reilly, S. Y., and N. Hayward, 2010, Lithospheric, Cratonic, and Geodynamic Setting of Ni-Cu-PGE Sulfide Deposits: Econ. Geol., **105**, 1057-1070.

Campbell, I. H., 2005, Large igneous provinces and the mantle plume hypothesis: Elements, **1**, 256-269.

Cawood, P. A., Wang, Y. J., Xu, Y. J., and G. C. Zhao, 2013, Locating South China in Rodinia and Gondwana: a fragment of greater India lithosphere?: Geology, **41**, 903-906.

Charvet, J., Shu, L. S., Faure, M., Choulet, F., Wang, B., Lu, H. F., and N. L. Breton, 2010, Structural development of the Lower Paleozoic belt of South China: genesis of an intracontinental orogen: J. Asian Earth Sci., **39**, 309-330.

Cloetingh, S., Burov, E., and T. Francois, 2013, Thermo-mechanical controls on intra-plate deformation and the role of plume-folding interactions in continental topography: Gondwana Res., **24**, 815-837.

Deng, Z. B., Liu, S. W., Zhang, L. F., Wang, Z. Q., Wang, W., Yang, P. T., Luo, P., and B. R. Guo, 2014, Geochemistry, zircon U–Pb and Lu–Hf isotopes of an Early Cretaceous intrusive suite in northeastern Jiangxi Province, South China Block: Implications for petrogenesis, crust/mantle interactions and geodynamic processes: Lithos, **200-201**, 334-354.

Fukao, Y., Obayashi, M., and T. Nakakuki, 2009, Deep Slab Project Group. Stagnant slab:a review: An. Rev. Earth Planet. Sci., **37**, 19-46.

Griffin, W. L., Begg, G. C., and S. Y. O'Reilly, 2013, Continental-root control on the genesis of magmatic ore deposits: Nat. Geosci., **6**, 905-909.

Goldfarb, R. J., Taylor, R. D., Collins, G. S., Goryachev, N. A. and O. F. Orlandini, 2014, Phanerozoic continental growth and gold metallogeny of Asia: Gondwana Research, **25**, 48-102.

Grabau, A. W., 1924, Migration of geosynclines: Bull. Geol. Soc. China, **3**, 207-349.

Hall, R., 2012, Late Jurassic–Cenozoic reconstructions of the Indonesian region and the Indian Ocean: Tectonophysics, **570-571,1-**41.

Hayden, L. A., and E. A. Watson, 2007, diffusion mechanism for core-mantle interaction: Nature, **450**, 709-711.

He, C. S., Dong, S. W., Santosh, M., and X. H. Chen, 2013, Seismic Evidence for a Geosuture between the Yangtze and Cathaysia Blocks, South China: Sci. Rep., **3**, 2200.

He, C. S., Dong, S. W., Santosh, M., Li, Q. S., and X. H. Chen, 2015, Destruction of the north China Craton: a perspective based on receiver function analysis: Geol. J., **50**, 93-103.

He, C. S., 2020, Upwelling mantle plume and lithospheric delamination beneath the North China Craton: Phys. Earth Planet. Inter., **306**, 106548.

He, C. S., and M. Santosh, 2016, Crustal evolution and metallogeny in relation to mantle dynamics: A perspective from P-wave tomography of the South China Block: Lithos, **263,3-**14.

He, C.S., and M. Santosh, 2021, Mantle upwelling beneath the Cathaysia Block, South China. Tectonics, https://doi.org/10.1029/2020TC006447.

Herzberg, C., and M. J. O'Hara, 2002, Plume-associated ultramafic magmas of Phanerozoic age: J. Petrol., **43**, 1857-1883.

Hu, R. Z., Mao, J. W., Fan, W. M., Hua, R. M Bi, X. W., Zhong, H., song, X. Y., and Y. Tao, 2010, Some scientific questions on the intra-continental metallogeny in the South China continent: Earth Sci. Front., **17**, 13-26 (in Chinese with English abstract).

Keith, M., 2001, Evidence for a plate tectonics debate: Earth-Sci. Rev., **55**, 235-336.

Khomich, V. G., Boriskina, N. G., and M. Santosh, 2014, A geodynamic perspective of world-class gold deposits in East Asia: Gondwana Res., **26**, 816-833.

Lei, J., 2012, Upper-mantle tomography and dynamics beneath the North China Craton: J. Geophys. Res., **117**, B06313.

Li, S. R., and M. Santosh, 2017, Geodynamics of heterogeneous gold mineralization in the North China Craton and its relationship to lithospheric destruction: Gondwana Res., **50**, 267-292.

Li, S. R., Santosh, M., Zhang, H. F., Shen, J. F., Dong, G. C., Wang, J. Z., and J. Q. Zhang, 2013, Inhomogeneous lithospheric thinning in the central North China Craton: zircon U–Pb and S–He–Ar isotopic record from magmatism and metallogeny in the Taihang Mountains: Gondwana Res., **23**, 141-160.

Li, S. Z., Santosh, M., Zhao, G. C., Zhang, G. W., and C. Jin, 2012, Intracontinental deformation in a frontier of super-convergence: A perspective on the tectonic milieu of the South China Block: J. Asian Earth Sci., **49**, 313-329.

Liu, L., Liu, L., Xu, Y. G., Xia, B., Ma, Q. and M. Menzies, 2019, Development of a dense cratonic keel prior to the destruction of the north China craton: constraints from sedimentary records and numerical simulation: J. Geophys. Res., **124**, 13192-13206

Lobkovsky, L., and V. Kotelkin, 2015, The history of supercontinents and oceans from the standpointof thermochemical mantle convection: Precambrian Res., **259**, 262-277.

Meert, J. G., 2012, What is in a name? The Columbia (Paleopangaea/Nuna) supercontinent: Gondwana Res., **21**, 987-993.

McInnes, B. I. A., McBride, J. S., Evans, N. J., Lambert, D. D., and A. S. Andrew, 1999, Osmium Isotope Constraints on Ore Metal Recycling in Subduction Zones: Science, **286**, 512-516.

Morgan, W.J., 1971. Convection plumes in the lower mantle: Nature, **230**, 42-43.

Muntean, J. L., Cline, J. S., Simon, A. C., and A. A. Longo, 2011, Magmatic–hydrothermal origin of Nevada's Carlin-type gold deposits: Nat. Geosci., **4**, 122-127.

Nance, R. D., Murphy, J. B., and M. Santosh, 2014, The supercontinent cycle: A retrospective essay: Gondwana Res., **25,4-**29.

Oppliger, G. L., Murphy, J. B., and G. H. Brimhall Jr. 1997, Is the ancestral Yellowstone hotspot responsible for the Tertiary "Carlin" mineralization in the Great Basin of Nevada?: Geology, **7**, 627-630.

Peacock, S. M., 1996, Thermal and petrologic structure of subduction zones. Geophys. Mon., **96**, 119-133.

Phillips, E. H., Sims, K. W. W., Blichert-Toft, J., Aster, R. C., Gaetani, G. A., Kyle, P. R., Wallace, P. J., and D. J. Rasmussen, 2018, The nature and

evolution of mantle upwelling at Ross Island, Antarctica, with implications for the source of HIMU lavas: Earth Planet. Sci. Lett., **498**, 38-53.

Pilidou, S., Priestley, K., Debayle, E., and ò. Gudmundsson, 2005, Rayleigh wave tomography in the North Atlantic: high resolution images of the Iceland, Azores and Eifel mantle plumes: Lithos, **79**, 453-474.

Pirajno, F., 2007, Ancient to modern earth: the role of mantle plume in the making of continental crust: Earth's Oldest Rocks, *in* M. J. V. Kranendonk, R. H. Smithies, and V. C. Bennett, eds., Developments in Precambrian Geology, 15.

Pirajno, F., and M. Santosh, 2015, Mantle plumes, supercontinents, intracontinental rifting and mineral systems: Precambrian Res., **259**, 243-261.

Santosh, M., Maruyama, S., and S. Omori, 2009, A fluid factory in solid Earth: Lithosphere, **1**, 29-33.

Santosh, M., Zhao, D. P., and T. M. Kusky, 2010, Mantle dynamics of the Paleoproterozoic North China Craton: a perspective based on seismic tomography: J. Geodyn., **49**, 39-53.

Shellnutt, J. G., 2014, The Emeishan large igneous province: A synthesis: Geosci. Front., **5**, 369-394.

Sisson, T. W., 2003, Native gold in a Hawaiian alkalic magma: Econ. Geol., **98**, 643-648.

Sun, T., 2006. The distribution of granites from South China and its petrogenesis: Geochim. Cosmochim. Ac., **70**, A626.

Sun, W. D., Ding, X., Hu, Y. H., and X. H. Li, 2007, The golden transformation of the Cretaceous plate subduction in the west Pacific: Earth Planet. Sci. Lett., **262**, 533-542.

Tassara, S., González-Jiménez, J. M., Reich, M., Schilling, M. E., Morata, D., Begg, G., Saunders, E., Griffin, W. L., O'Reilly, S. Y., Grégoire, M., Barra, F., and A. Corgne, 2017, Plume-subduction interaction forms large auriferous provinces: Nat. Geosci., **8**, 1-7.

Trubitsyn, V. P., 2019, Gravitational Differentiation in the Regimes from Stokes Settling to Rayleigh–Taylor Flows: Izv. Phys. Solid Earth, **55**, 205-217.

Webber, A. P., Roberts, S., Taylor, R. N., and I. K. Pitcairn, 2013, Golden plumes: Substantial gold enrichment of oceanic crust during ridge-plume interaction: Geology, **41**, 87-90.

Weis, D., Garcia, M. O., Rhodes, J. M., Jellinek, M., and J. S. Scoates, 2011, Role of the deep mantle in generating the compositional asymmetry of the Hawaiian mantle plume: Nat. Geosci., **4**, 831-838.

Wilson, J. T., 1963, A possible origin of the Hawaiian Islands: Canadian J. Phys., **41**, 863-870.

Wu, F. Y., Yang, J. H., Xu, Y. G., Wilde, S. A., and R. J. Walker, 2019, Destruction of the North China Craton in the Mesozoic: Ann. Rev. Earth Planet. Sci., **47**, 173-195.

Yan, Y., Hu, X. Q., Lin, G., Santosh, M., and L. S. Chan, 2011, Sedimentary provenance of the Hengyang and Mayang basins, SE China, and implications for the Mesozoic topographic change in South China Craton: Evidence from detrital zircon geochronology: J. Asian Earth Sci., **41**, 494-503.

Yang, J. H., Wu, F. Y., and S. A. Wilde, 2003, A review of the geodynamic setting of large-scale Late Mesozoic gold mineralization in the North China Craton: an association with lithospheric thinning: Ore Geol. Rev., **23**, 125-152.

Yao, J. L, Shu, L. S., and M. Santosh, 2011, Detrital zircon U–Pb geochronology, Hf-isotopes and geochemistry—New clues for the Precambrian crustal evolution of Cathaysia Block, South China: Gondwana Res., **20**, 553-567.

Yin, C. Q., Lin, S. F., Davis, D. W., Zhao, G. C., Xiao, W. J., Li, L. M., and Y. H. He, 2013, 2.1–1.85Ga tectonic events in the Yangtze Block, South China: Petrological and geochronological evidence from the Kongling Complex and implications for the reconstruction of supercontinent Columbia: Lithos, **182-183**, 200-210.

Zhai, M. G., Fan, Q. C., Zhang, H. F., Sui, J. L., and J. A. Shao, 2007, Lower crustal processes leading to Mesozoic lithospheric thinning beneath eastern North China: Underplating, replacement and delamination: Lithos, **96**, 36-54.

Zhai, Y. S., Miao, L. C., Xiang, Y. C., Deng, J., and J. P. Wang, 2002, Preliminary discussion on gold ore forming system in greenstone belt-type of North China Craton: Earth Sci. J., **27**, 522-531 (In Chinese with English abstract).

Zhang, H. F., Sun, M., Zhou, X. H., Fan, W. M., Zhai, M. G., and J. F. Yin, 2002, Mesozoic lithosphere destruction beneath the North China Carton: evidence from major-traceelement and Sr–Nd–Pb isotope studies of Fang Cheng basalts. Contrib: Mineral. Petr., **144**, 241-253.

Zhao, P., Appel, E., Xu, B. and T. Sukhbaatar, 2020, First paleomagnetic result from the Early Permian volcanic rocks in northeastern Mongolia: Evolutional implication for the Paleo-Asian Ocean and the Mongol-Okhotsk Ocean: J. Geophys. Res., **125**, e2019JB017338.

Zhao, D., 2001, Seismic structure and origin of hotspots and mantle plumes: Earth Planet. Sci. Lett., **192**, 251-265.

Zhao, D., 2004, Global tomographic images of mantle plumes and subducting slabs: Insight into deep Earth dynamics: Phys. Earth Planet. Int., **146,3-**34.

Zhao, D., and E. Ohtani, 2009, Deep slab subduction and dehydration and their geodynamic consequences: evidence from seismology and mineral physics:

Gondwana Res., **16**, 401-413.

Zhao, G. C., and M. G. Zhai, 2013, Lithotectonic elements of Precambrian basement in the North China Craton: review and tectonic implications: Gondwana Res., **23**, 1207-1240.

Zhao, L., and T. Y. Zheng, 2005, Using shear wave splitting measurement to investigate the upper mantle anisotropy beneath the North China Craton: distinct variation from east to west: Geophys. Res. Lett., **32**, L1039.

Zhao, Z. F., and Y. F. Zheng, 2009, Remelting of subducted continental lithosphere: petrogenesis of Mesozoic magmatic rocks in the Dabie–Sulu orogenic belt: Sci. China Seri. D, **52**, 1295-1318 (in Chinese with English abstract).

Zheng, Y. F., Xiao, W. J., and G. C. Zhao, 2013, Introduction to tectonics of China: Gondwana Res., **23**, 1189-1206.

Zhou, X. M., Sun, T., Shen, W. Z., Shu, L. S., and Y. L. Niu, 2006, Petrogenesis of Mesozoic granitoids and volcanic rocks in South China: a response to tectonic evolution: Episodes, **29**, 26-33.

Zhu, J., Zhang, Z. C., Santosh, M., and Z. L. Jin, 2020, Carlin-style gold province linked to the extinct Emeishan plume: Earth Planet. Sci. Lett., **530**, 115940.

Figure captions

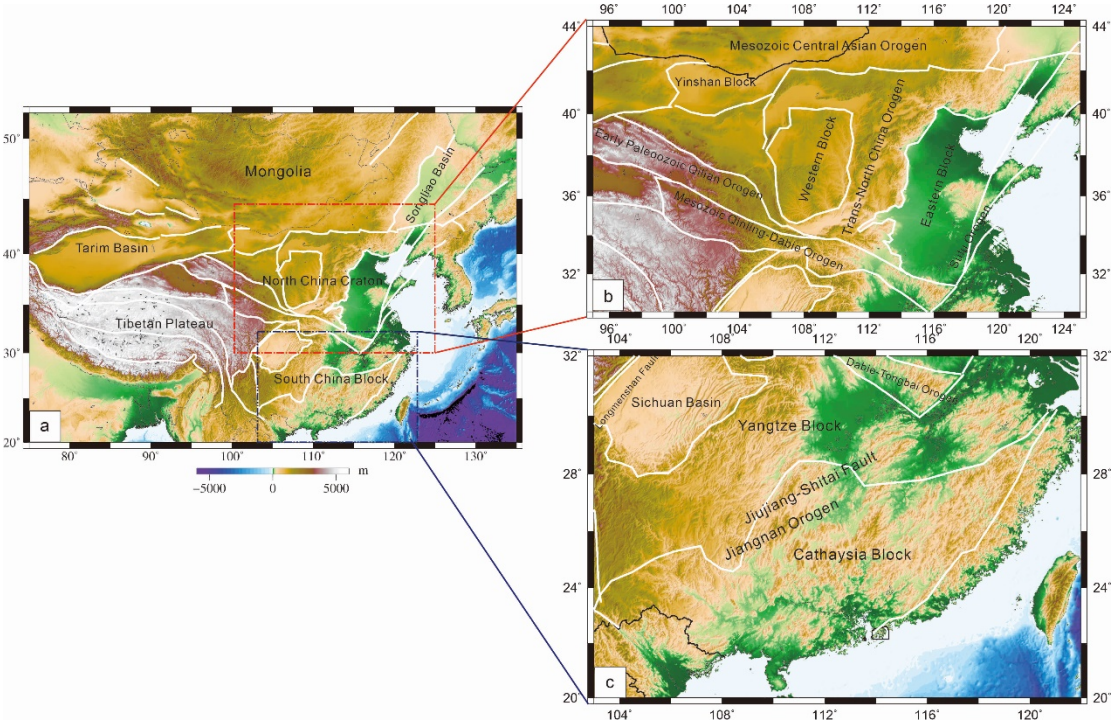

Fig. 1. The location of the study region (a): left panel. Red rectangle: North China Block (Craton). Blue rectangle: South China Block. Upper figure of right panel (b): the tectonic formwork of the NCC. Lower figure of right panel (c): the tectonic formwork of the SCB. White lines: tectonic boundaries.

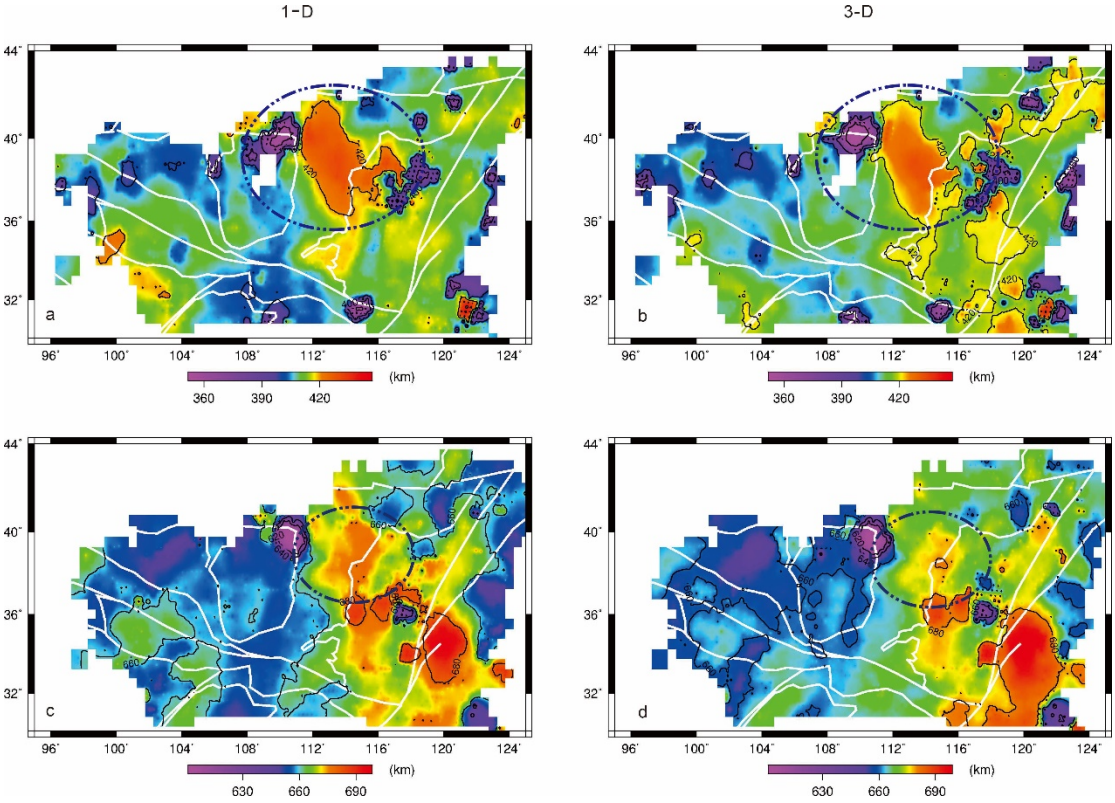

Fig. 2. CCP stacking of receiver functions. Both the 410 km discontinuity (a, b) and the 660 km discontinuity (c, d) deepen by approximately 15 and 20 km (blue circles) and represent a vestige of an upwelling mantle plume in the NCC. Left panels: results corrected using the AK135 1-D velocity model (a, c). Right panels: results corrected using the 3-D velocity model (b, d) inferred tomography (He, 2020).

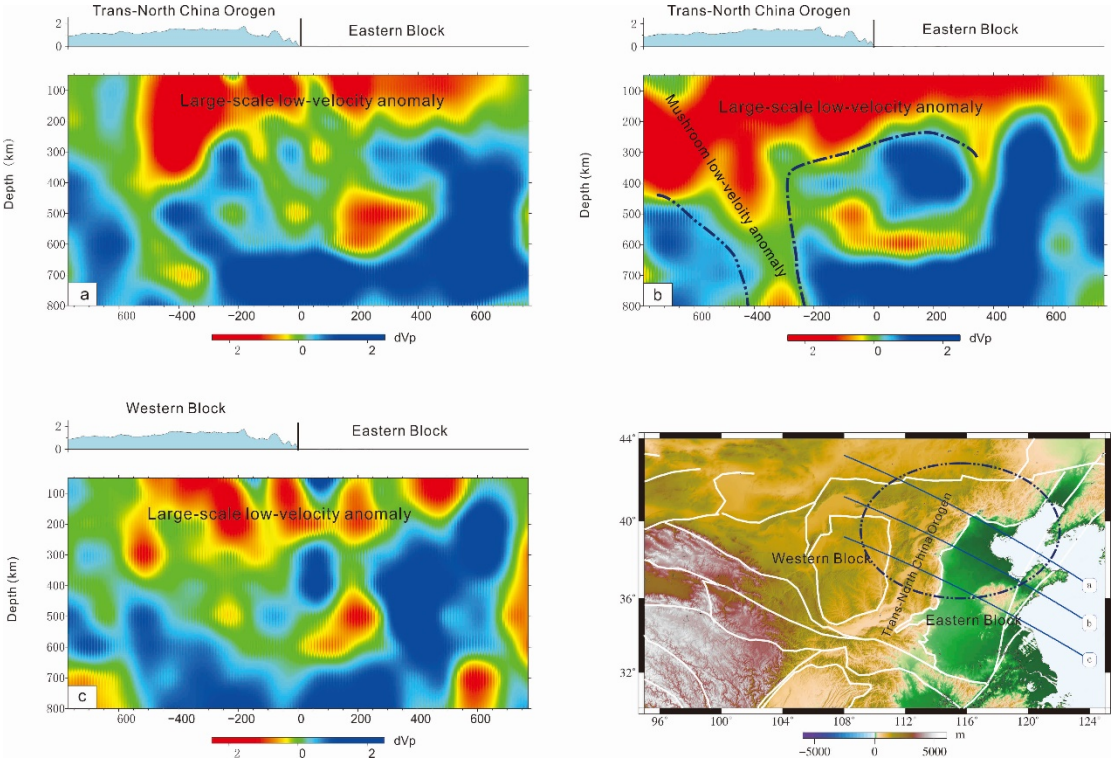

Fig. 3. P-wave velocity perturbations (He, 2020). Mushroom-like low-velocity anomaly might be related to an upwelling mantle plume (b). Blue oval: the region influenced by the upwelling mantle plume.

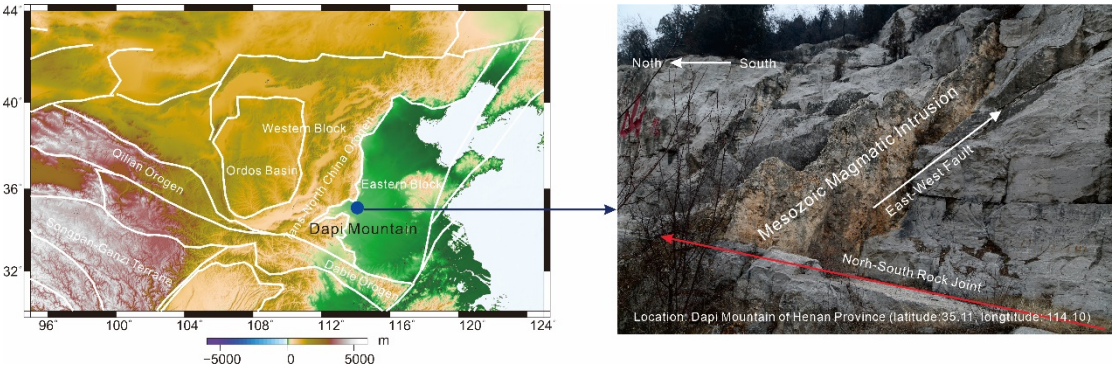

Fig. 4. Example of Mesozoic magmatic intrusion in the Eastern Block of the NCC (the photograph in the right panel was taken by Chuansong He in the Dapi Mountain of Henan Province).

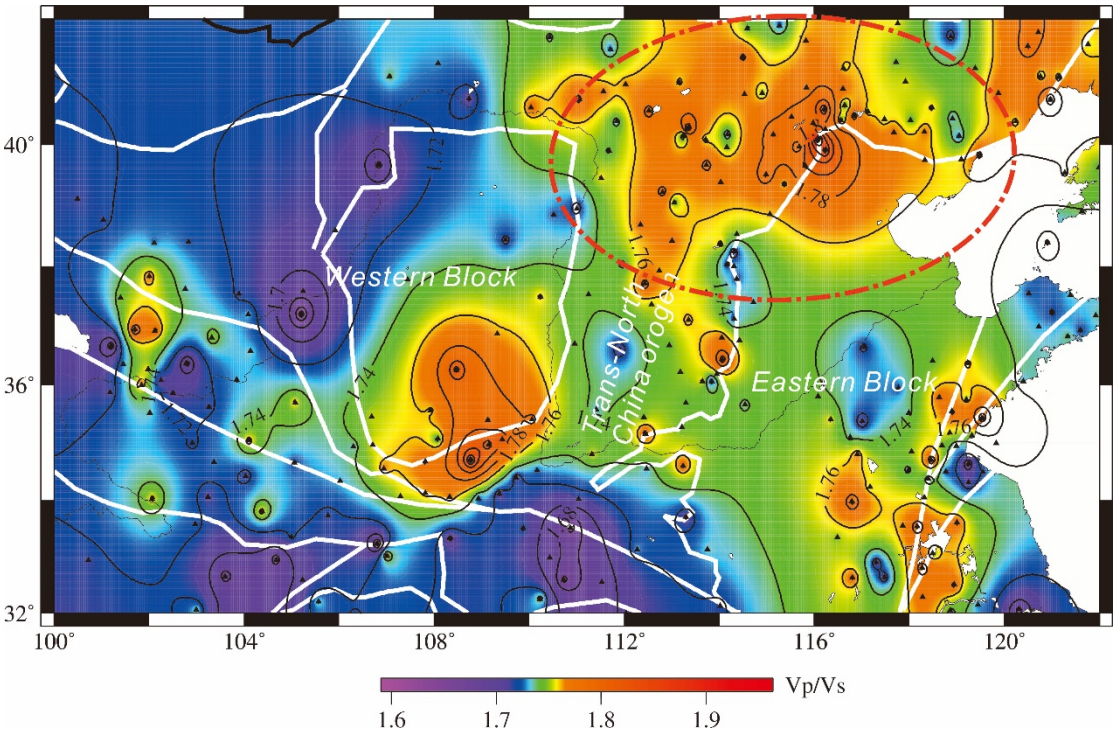

Fig. 5. Distribution of the Vp/Vs ratio in the NCC. Red oval: underplating region, which has higher Vp/Vs ratios (Vp/Vs ratio is greater than 1.76) (He et al., 2015).

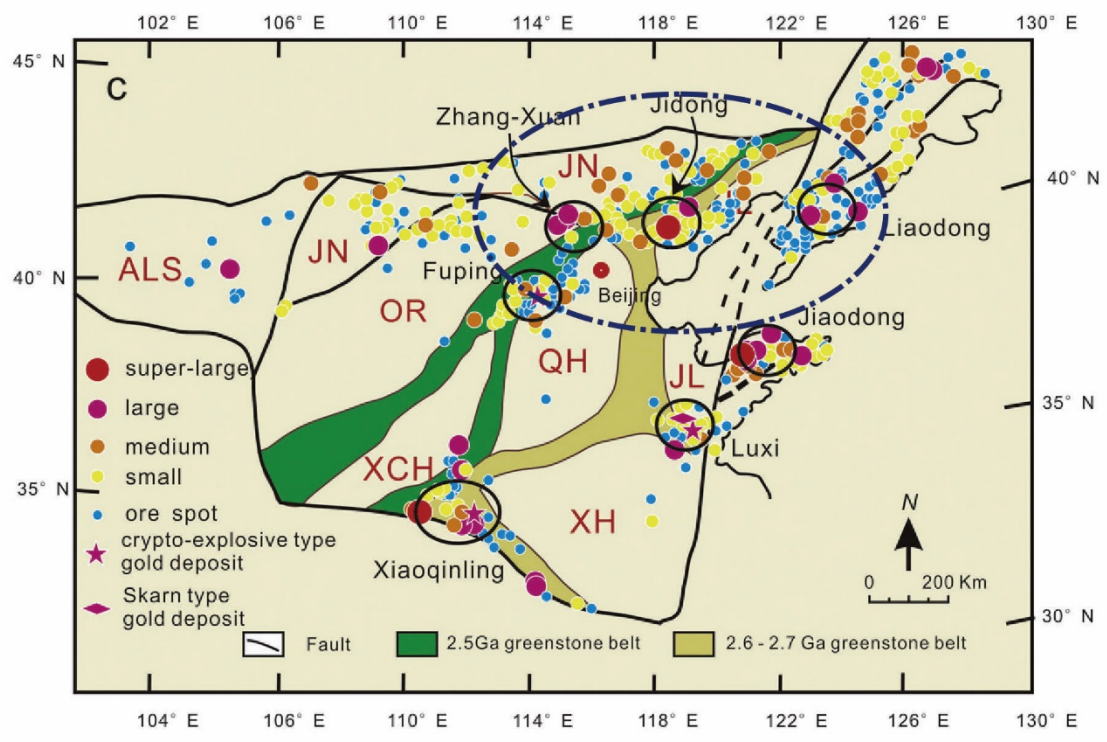

Fig. 6. Circle: site of gold mineralization. The gold mineral distribution (Li et al., 2017) corresponds to the location of magmatic underplating and the upwelling mantle plume (blue oval).

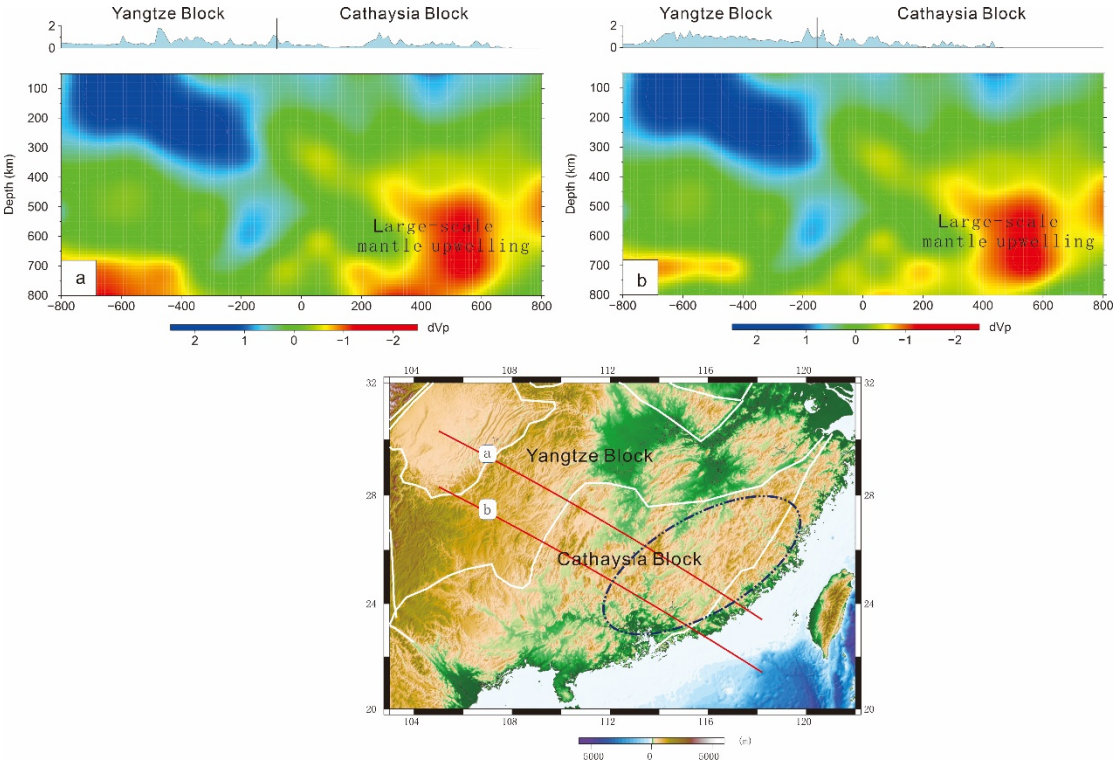

Fig. 7. P-wave velocity perturbations (He and Santosh, 2016). Large-scale mantle upwelling beneath the Cathaysia Block. Blue oval: the location of large-scale mantle upwelling.

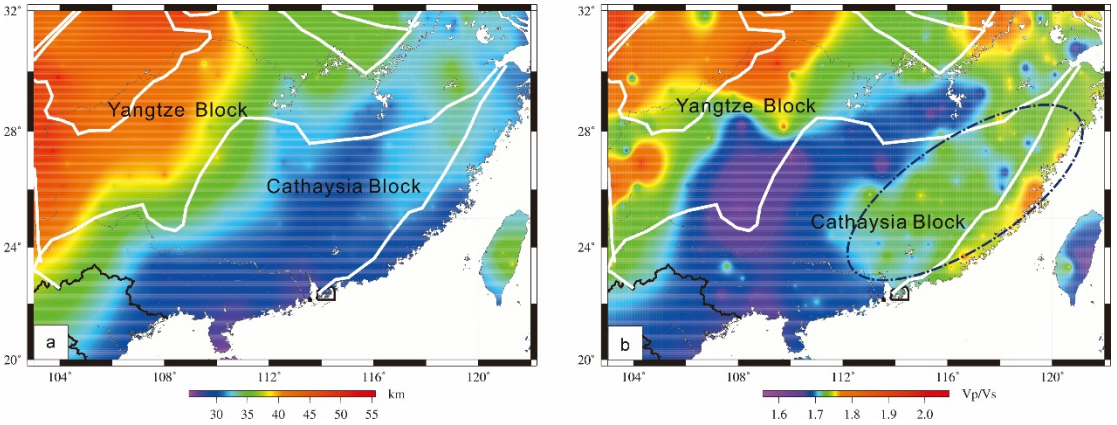

Fig. 8. Crustal thickness (a) and Vp/Vs ratio (b) (He et al., 2013). The Cathaysia Block has a uniform crustal thickness. Blue oval: relatively high Vp/Vs ratio, which is less than 1.76, corresponding to the location of the upwelling mantle.

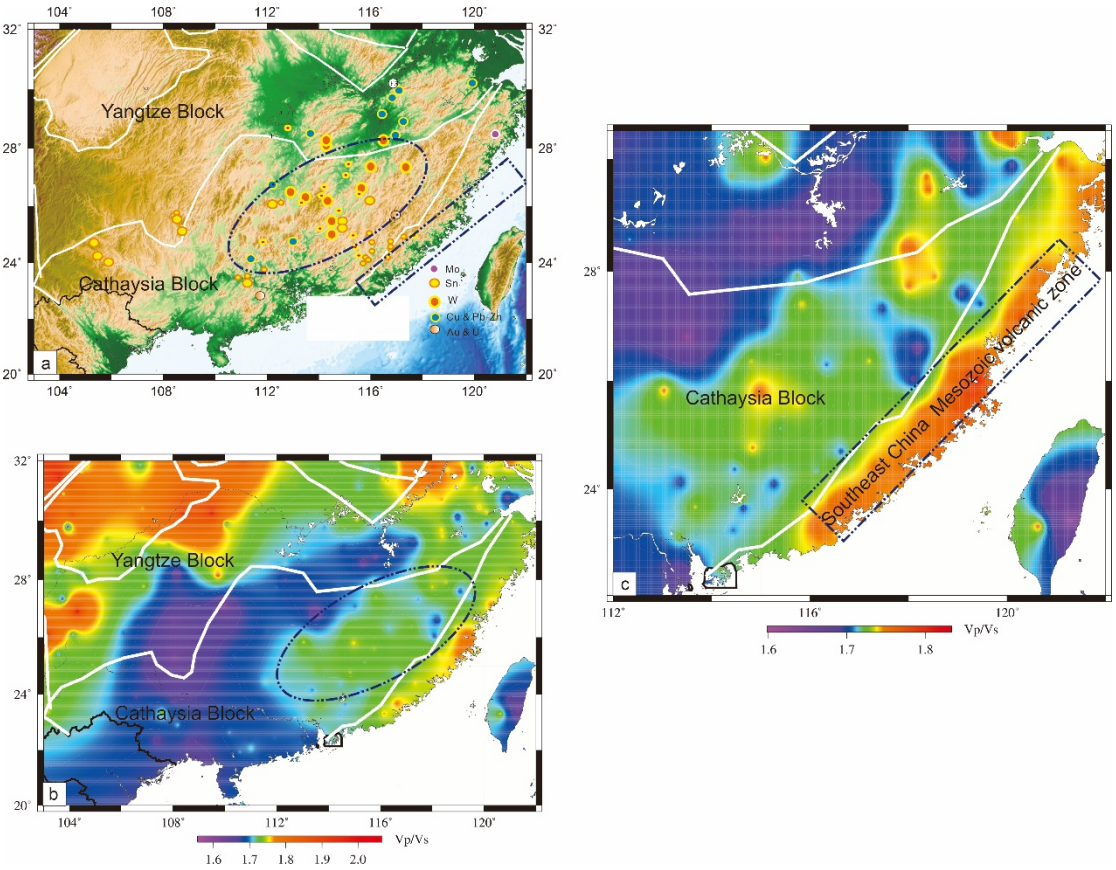

Fig. 9. Regions with high Vp/Vs ratios and metal deposits zones. The Mesozoic volcanic zone in Southeast China (the area with high Vp/Vs ratios) (Fig. 9c, rectangle) corresponds with the continental margin metal deposit zone (Cretaceous Sn-W-Pb-Zn-Au-U system along the continental margin) (Fig. 9a, rectangle). Another area with high Vp/Vs ratios (Fig. 9b, blue oval) corresponds with the Nanling metal deposit zone (Nanling belt and adjacent area, a granite-related W-Sn-Mo-Bi-Be system formed from 160-150 Ma) (Fig. 9a, blue oval).